Spectral Estimation of Received Phase in the Presence of Amplitude Scintillation

V. A. Vilnrotter, D. H. Brown, and W. J. Hurd
Communications Systems Research Section

A technique is demonstrated for obtaining the spectral parameters of the received carrier phase in the presence of carrier amplitude scintillation, by means of a digital phase locked loop. Since the random amplitude fluctuations generate time-varying loop characteristics, straightforward processing of the phase detector output does not provide accurate results. The method developed here performs a time-varying inverse filtering operation on the corrupted observables, thus recovering the original phase process and enabling accurate estimation of its underlying parameters.

I. Introduction

The purpose of this article is to present a method for estimating the power spectral density of the phase of a received carrier, when there is significant amplitude scintillation on the received waveform. For example, these conditions occur when the spacecraft transmits through the solar corona. Knowledge of the phase spectrum is important for improving carrier tracking through bandwidth optimization, or through more sophisticated real-time adaptive techniques.

In a previous article [1] we reported the results of an experiment, carried out at DSS 14 at Goldstone, where the DSN Advanced Receiver was used to track weak signals originating from the Pioneer 10 spacecraft on its way out of the solar system [2]. One purpose of the experiment was to optimize the bandwidth of the Advanced Receiver's coherent phase-locked loop in near-real time, thus minimizing the root mean square (rms) phase error and improving the quality of the recovered data. The optimization was based on estimates of the phase spectral density and the spectral level of the additive noise, using a robust ad hoc estimator. Amplitude fluctuation was not a factor in that experiment. More recently, an attempt was made to track Voyager 2, as it travelled behind the solar corona in the latter part of December 1987 [3]. A maximum likelihood estimator was developed to obtain improved estimates. However, the unexpectedly large amplitude fluctuations encountered near the Sun rendered these parameter estimates questionable, even though phase lock was maintained with the help of the ad hoc estimator. A large amount of data was collected and subsequently analyzed. In this article, we present the results of the data analysis and demonstrate a technique for obtaining estimates of the relevant spectral parameters, taking into account the effects of the time-varying amplitude. Our ultimate goal is to adaptively control loop parameters for the purpose of minimizing phase error, even in the presence of severe amplitude fluctuations.

Radio waves propagating through a turbulent medium, such as the solar corona, undergo random changes that often alter their characteristics. From the viewpoint of deep space com-

munications, the most significant of these effects are phase and amplitude scintillation, spectral and angular broadening, and Faraday rotation [4]. Amplitude and phase scintillation are the most pronounced effects at the 8.4-GHz carrier frequency (X-band) employed by the DSN. Scintillations are caused by random inhomogeneities within the propagation channel. Amplitude scintillation is basically a diffraction phenomenon, caused by plasma irregularities that are smaller than or roughly equal to the Fresnel zone size at the irregularity. The time scale of the amplitude fluctuations due to the solar corona is typically on the order of a second. Phase scintillation is primarily a refraction effect, caused by plasma irregularities with different refractive indexes, and different random velocity components along the line of sight. The power spectral densities of both phase and amplitude fluctuations obey inverse power relations in certain frequency regions near the carrier frequency, which means that the level of the spectral density is inversely proportional to the frequency difference, raised to some constant power

$$S(f) \simeq S_1 |f|^{-\alpha} \tag{1}$$

For phase spectra, the exponent α due to the solar corona is typically 8/3 or less at small Sun-Earth-probe (SEP) angles [5]. The coefficient S_1 is the value of the spectral level at a frequency of 1 Hz from the carrier. Oscillator instabilities aboard the spacecraft also generate a power law type spectral density, but with an exponent of $\alpha = 3$ [6]. In the current application, we shall assume that plasma effects dominate, and model the spectral density of the phase fluctuations as in Eq. (1) in order to obtain the required parameter estimates. However, care must be exercised in interpreting the results, since other effects (such as oscillator instability) may not be completely negligible. The spectral characteristics of the amplitude fluctuations are less critical, since only the bandwidth of the amplitude fluctuations will be used to estimate the scintillating amplitude.

II. The Received Waveform

As the transmitted signal propagates through the solar plasma, it suffers random amplitude and phase distortions that degrade the quality of the received waveform. An accurate description of these degradations is the subject of the following paragraphs.

A. Signal and Noise Representations

Having propagated through the turbulent channel, the residual component of the transmitted radio wave $s(t)$ can be represented at the receiver as

$$s(t) = \sqrt{2}\, A(t) \cos(\omega_0 t + \theta(t)) \tag{2}$$

where ω_0 is the carrier frequency in radians per second, $A(t)$ is a random amplitude function describing the channel-induced amplitude scintillation, and $\theta(t)$ is a random phase process, also due to the channel. Unfortunately, a perfect measurement of this received waveform cannot be made, because of background radiation and receiver noise. Within the frequency band of interest, the sum of all significant noise contributions can be modeled as an equivalent narrowband Gaussian process, with representation

$$n(t) = \sqrt{2}\, [n_c(t) \cos(\omega_0 t) - n_s(t) \sin(\omega_0 t)] \tag{3}$$

Here $n_c(t)$ and $n_s(t)$ are taken to be independent white Gaussian processes, each with two-sided spectral level $N_0/2$, within the frequency band of interest. Thus, the receiver observes the channel-corrupted signal in the presence of additive white Gaussian noise:

$$r(t) = s(t) + n(t) \tag{4}$$

Amplitude and phase information may be extracted from the received waveform by means of coherent processing techniques, such as by means of a phase-locked loop in a coherent receiver. A coherent receiver estimates the total phase $(\omega_0 t + \theta(t))$, and multiplies the received waveform $r(t)$ by locally generated sinusoids driven by the estimated phase process $\hat{\theta}(t)$. If the estimate is a good approximation to the received phase, then the resulting baseband waveforms can be represented as

$$r_I(t) = A(t) \cos(\phi(t)) + n_I(t) \tag{5a}$$

$$r_Q(t) = A(t) \sin(\phi(t)) + n_Q(t) \tag{5b}$$

where $\phi(t) = \theta(t) - \hat{\theta}(t)$ is the instantaneous phase error, and $n_I(t)$ and $n_Q(t)$ are approximately white Gaussian processes with two-sided spectral level $N_0/2$, independent of each other and of the underlying phase error (this last assumption is valid only if the correlation time of the additive noise is short compared to that of the phase process). The I (or in-phase) signal can be used for amplitude estimation, whereas the Q (or quadrature) signal is generally used for phase control. Note that if the phase estimate is accurate so that $|\phi(t)| \ll 1$, then Eqs. (5a) and (5b) reduce to

$$r_I(t) \simeq A(t) + n_I(t) \tag{6a}$$

$$r_Q(t) \simeq A(t)\, \phi(t) + n_Q(t) \tag{6b}$$

In particular, the scintillating amplitude $A(t)$ can be estimated under this condition, since the in-phase signal $r_I(t)$ reduces

to the sum of the amplitude function and the equivalent noise, independent of the phase process.

In digital systems, the analog waveforms are converted to numerical sequences prior to processing. The conversion operation is called sampling. It is generally implemented by averaging the analog waveform over intervals that are short compared to the correlation time of the desired component, or by performing other roughly equivalent operations. For purposes of analysis it is convenient to adopt the averaging approach, and model the received samples as

$$r_x(i) = \frac{1}{T}\int_{t_i}^{t_i+T} r_x(t)\,dt = s_x(i) + n_x(i) \qquad (7)$$

where x represents either I or Q, $s_I(i) = A(i)$, and $s_Q(i) = A(i)\,\phi(i)$. If the noise correlation time is short compared to the averaging time T, then the variance of either noise sample becomes $N_0/2T$, while its mean value remains zero. It is often necessary (or desirable) to resample the original sequence at various points within the system by averaging consecutive samples. Because integration is a linear operation, this type of resampling is exactly equivalent to averaging the analog waveform over the longer (resampled) time interval. Thus, if L consecutive samples are averaged, the variance of either resulting noise sample becomes $N_0/2LT$. The desired signal component remains essentially undistorted by resampling, provided its correlation time exceeds LT by a significant margin.

B. Amplitude Scintillation Spectrum

An example of a scintillating radio wave observed in the presence of additive noise was provided by the Voyager 2 spacecraft as it passed behind the solar corona. As an example, we use the data from day-of-year (DOY) 357, corresponding to an SEP angle of about 2.3 degrees, because strong amplitude scintillations were evident. The Advanced Receiver tracked the phase with small error, validating our linear model.

The received analog waveform was initially sampled at approximately 10 million samples/s, then summed and resampled at a rate of 320 samples/s, yielding a sampling time of $T = 3.125$ ms. This was the update rate of the digital phase locked loop. The observables generated by the coherent loop were further summed and resampled at 40 samples/s, corresponding to a final resampling time of $LT = 0.025$ second.

A sample sequence of the observables, consisting of 256 consecutive samples, is shown in Fig. 1, spanning a time of 6.4 seconds. The discrete sample values are connected with straight line segments to aid in visual perception. Slow variations in the average amplitude are apparent. The significant frequency components of this sequence can be quantified by estimating its power spectral density. This was done by means of averaged periodograms, described in detail in Section IV. Periodograms can be obtained efficiently using fast Fourier-transform (FFT) algorithms. The normalized spectral density estimate of the amplitude shown in Fig. 2 was obtained by averaging 100 disjoint sequences of 256 samples each, and dividing by the zero-frequency value. It is apparent that the spectrum can be divided into two distinct regions, namely a "high-frequency" region due to the white noise where the spectrum appears flat, and a "low-frequency" region where the signal amplitude fluctuations dominate.

An estimate of the amplitude fluctuations may be obtained in real time by passing the received sequence through a low-pass filter with bandwidth great enough to ensure acceptably small distortion in the scintillation spectrum. The required filtering operation can be generated by averaging K consecutive samples in a "sliding window" implementation. We take the bandwidth of this filter to be the frequency of the first null, namely

$$B_{FN} = (LTK)^{-1} \qquad (8)$$

(Note this is greater than the usual "–3 dB" bandwidth.) Observing that there is no significant power in the amplitude scintillations above 2 Hz, we set $B_{FN} = 2$ Hz, for which $K = 1/(2TL) = 20$. The estimated amplitude function $\hat{A}(i)$ is shown in Fig. 1, while the spectrum of the filtered estimates is shown in Fig. 2, both represented by dashed curves. The performance of this rather simple amplitude estimator is not expected to be as good as that of more sophisticated algorithms based on optimum estimation principles. However, since the sliding window combines ease of implementation with acceptable performance, it is considered adequate for the purpose of demonstrating the concepts developed in this article.

III. Separation of Amplitude and Phase Effects

In this section we describe a technique for reconstructing the noise-corrupted phase process from the recorded phase detector output, effectively removing the random coefficient of the phase due to the scintillating amplitude. First we discuss the standard digital phase locked loop (PLL), then we model the loop in the presence of random signal-amplitude variations, and finally we demonstrate the reconstruction of the received phase.

A. Linear Time Invariant Phase Locked Loop

The quadrature samples defined in the previous section are used in the Advanced Receiver to drive a digital phase-locked loop, which in turn generates estimates of the received phase process at the loop update rate. These estimates control the frequency of a local oscillator operating at, or near, the received carrier frequency, whose output is used to perform the desired downconversion operation. With little loss in generality, we shall assume that direct baseband downconversion is performed. If the loop is locked, and operating with small instantaneous phase error most of the time, then the linear model yields an accurate description of loop operation.

A linear model of the digital phase-locked loop is shown in Fig. 3. The loop generates estimates of the received phase sequence, $\hat{\theta}(i)$, and subtracts these estimates from the received phase sequence $\theta(i)$. The received phase consists of three independent components: a doppler-induced phase process $d(i)$, transmitter instability $\psi_t(i)$, and a plasma-induced phase process $\psi_p(i)$. Therefore we can write $\theta(i) = d(i) + \psi_t(i) + \psi_p(i)$. The instantaneous phase error, defined as $\phi(i) = \theta(i) - \hat{\theta}(i)$, is multiplied by a slowly varying sequence $A(i)$ representing the plasma-induced amplitude scintillation of the received carrier. After adding the equivalent noise sequence $n_Q(i)$, the resulting sequence is filtered by the loop filter. The filtered error sequence $e(i)$ controls the frequency of a numerically controlled oscillator (NCO) whose output is also considered to be a phase sequence, sampled at the same rate as the input. The phase estimate is the sum of the NCO phase plus an independent random sequence representing NCO drift. The observable sequence is denoted by $w(i)$. It is a resampled version of the phase detector sequence which appears at the input to the loop filter. Henceforth we assume that $w(i) \simeq y(i)$, because in our case the resampling rate is much greater than the bandwidth of the phase process.

B. PLL With Time Varying Signal Amplitude

In analogy with Heaviside's differential operator, it is convenient to define the shift operator S, which operates on an arbitrary sample $x(i)$ according to the rule

$$S^{-k}x(i) = x(i-k) \tag{9}$$

The shift operator allows us to relate the output of a linear filter, defined by the operator $P(S)$, to its input as $y(i) = P(S)\,x(i)$. Since the z-transform of a k-increment delay is z^{-k}, it follows that the transfer function of the above filter in the z-domain is $P(z)$. Making use of the shift-operator concept, the digital loop equations become

$$\phi(i) = \theta(i) - \hat{\theta}(i) \tag{10a}$$

$$y(i) = A(i)\,\phi(i) + n_Q(i) \tag{10b}$$

$$\hat{\theta}(i) = F(S)\,N(S)\,y(i) + \psi_r(i) \tag{10c}$$

Defining the total phase process $\xi(i) = d(i) + \psi_t(i) + \psi_p(i) - \psi_r(i)$, Eq. (10) can be solved for the phase error, hence the phase detector output, as

$$\phi(i) = \left\{1 + A(i)F(S)N(S)\right\}^{-1}\xi(i) + \left\{\frac{A(i)F(S)N(S)}{1 + A(i)F(S)N(S)}\right\}\frac{n_Q(i)}{A(i)} \tag{11a}$$

$$y(i) = A(i)\left\{1 + A(i)F(S)N(S)\right\}^{-1}\left[\xi(i) + \frac{n_Q(i)}{A(i)}\right] \tag{11b}$$

Thus, the phase detector output contains a term that depends on the phase $\xi(i)$, and one that depends on the additive noise.

C. Reconstruction of the Phase Process

We observe that in Eqs. (11a) and (11b) both the phase and additive noise processes are operated on by time-varying operators, due to the fluctuating amplitude $A(i)$. Since the amplitude fluctuations vary slowly compared to both the loop response time and noise correlation time, and since estimates of the amplitude process are available, we may attempt to reconstruct the original processes by passing the phase detector output through a time-varying inverse filter of the form

$$P(S) = \frac{\{1 + \hat{A}(i)F(S)N(S)\}}{\hat{A}(i)} \tag{12a}$$

If $v(i)$ denotes the response of $P(S)$ to $y(i)$, the operation of the filter may be described by the recursion

$$v(i) = \sum_{l=0}^{4} a_l(i)\,y(i-l) + \sum_{l=1}^{2} b_l(i)\,v(i-l) \tag{12b}$$

The coefficients are derived in the Appendix. The filter's response to the phase detector output is

$$v(i) = \left\{\frac{1 + \hat{A}(i)F(S)N(S)}{\hat{A}(i)}\right\}y(i) \simeq \xi(i) + \left(\frac{n_Q(i)}{\hat{A}(i)}\right) \tag{13}$$

This is an estimate of the total phase process corrupted by a modified noise sequence. That this noise sequence is also white

follows from the following argument: over a suitably short time interval, such that channel statistics remain fixed, we can express the amplitude fluctuations as the sum of an average value plus a zero-mean random process

$$\hat{A}(i) = \bar{A} + n_A(i) = \bar{A}\left(1 + \frac{n_A(i)}{\hat{A}}\right) \tag{14a}$$

The modified noise sequence now becomes

$$\frac{n_Q(i)}{\hat{A}(i)} = \frac{n_Q(i)}{\bar{A}\left[1 + \frac{n_A(i)}{\bar{A}}\right]} = \frac{n_Q(i)}{\bar{A}}\left[1 - \frac{n_A(i)}{\bar{A}} + \frac{n_A^2(i)}{\bar{A}^2} - + \cdots\right]$$

$$\triangleq \frac{n_Q(i)\, n_{eq}(i)}{\bar{A}} \tag{14b}$$

where $n_{eq}(i)$ is the series inside the brackets. Assuming that the additive noise is independent of the amplitude process, the autocorrelation function of the modified noise sequence is

$$R_{\left(\frac{n_Q}{\hat{A}}\right)}(k) = (\bar{A})^{-2} R_{n_Q}(k) R_{n_{eq}}(k) \tag{15}$$

For uncorrelated noise samples we have $R_{n_Q}(k) = (N_0/2)\,\delta(k)$, which reduces Eq. (15) to

$$R_{\left(\frac{n_Q}{\hat{A}}\right)}(k) = (\bar{A})^{-2}\left(\frac{N_0}{2}\right) R_{n_{eq}}(0)\,\delta(k) \triangleq \frac{N_{0E}}{2}\,\delta(k) \tag{16}$$

Therefore $n_Q(i)/\hat{A}(i)$ is white, with a spectral level corresponding to the coefficient of the Kroenecker delta function. The power spectral density of the reconstructed observables consists of spectral contributions from both the phase and the modified noise processes:

$$S_v(f) \simeq S_\xi(f) + \frac{N_{0E}}{2} \tag{17}$$

In our application, the contributions of Doppler and receiver phase processes are small. The main components of the phase process are due to the solar corona and to transmitter oscillator instabilities. Both effects produce a power-law type phase spectrum near the carrier frequency, the first with exponent 8/3 or less, and the second with exponent 3. Thus we expect the observed spectral density to be composed of a constant spectral level due to the inverse-filtered white noise, plus a power law component due to the dominant phase process.

The estimated power spectral density for the data sequence under consideration is shown in Fig. 4. The white noise component is clearly evident. This figure is discussed further in the next section where we consider the problem of estimating the relevant channel parameters from the reconstructed sequence. These estimates may be used to monitor channel conditions, or to adaptively match receiver parameters to channel conditions for improved performance.

IV. Parameter Estimation

In this section we estimate the parameters of the spectral density of the received phase. First we discuss the method used to estimate the spectral density, and then describe the maximum likelihood (ML) algorithm used to estimate its parameters.

A. Power Spectral Density Estimation

An extensive body of literature exists on spectral estimation algorithms. Here we use a simple but well established approach known as Bartlett's procedure [7]. This technique is easy to implement, but yields good results whenever spectral resolution requirements are met with a small fraction of the available samples. In particular, estimates of the power spectral density are obtained by averaging independent periodograms, which can be generated by means of efficient FFT algorithms.

The periodogram of length N, $I_N(\omega)$, associated with the sequence $v(i)$, is defined as

$$I_N(\omega) = \frac{1}{N}\left|V(e^{j\omega})\right|^2 \tag{18a}$$

where

$$V(e^{j\omega}) = \sum_{i=0}^{N-1} v(i)\, e^{-j\omega i} \tag{18b}$$

is the discrete Fourier transform of the sequence $v(i)$. The use of periodograms in spectral estimation is justified on the grounds that in the limit as N approaches infinity, the expected value of the periodogram approaches the desired power spectral density. With $R_v(m)$ the autocorrelation function of v, we have from [7] that if $R_v(m) = 0$ for all $m > m_0$, then

$$\lim_{N\to\infty} E\{I_N(\omega)\} = \lim_{N\to\infty} \sum_{m=-(N-1)}^{N-1} \left(1 - \frac{|m|}{N}\right) R_v(m)\, e^{-j\omega m}$$

$$= S_v(\omega) \tag{19}$$

The FFT generates samples of the periodogram, evaluated at the points $\omega = 2\pi k/N$. With

$$V(k) = V(e^{j\omega})\Big|_{\omega = 2\pi k/N} \tag{20a}$$

it follows that

$$I_N(k) = I_N(\omega)\Big|_{\omega = 2\pi k/N} \tag{20b}$$

Suppose the observed samples were obtained from a white Gaussian process, and therefore are jointly Gaussian random variables with the autocorrelation function $R_v(m) = R_v(0)\,\delta(m)$. Consequently, the transformed samples $V(k)$ become complex Gaussian random variables. The correlation between the transformed samples at frequencies corresponding to k and l can be evaluated directly from the expression

$$\frac{1}{N}\overline{V(k)\,V^*(l)} = \frac{1}{N}\sum_{i=0}^{N-1}\sum_{n=0}^{N-1}\overline{v(i)\,v(n)}\; e^{-j\frac{2\pi}{N}(ki-ln)}$$

$$= \begin{cases} R_v(0) & ; \quad k = l \\ 0 & ; \quad k \neq l \end{cases} \tag{21}$$

where $*$ denotes conjugation, and the overbar denotes the expectation operator. It follows from Eq. (21) that the frequency samples are uncorrelated, hence independent by the Gaussian assumption. Since for $k = l$ the correlation expression corresponds to the expected value of the periodogram, we conclude that for white processes the periodogram is an unbiased estimator of spectral level.

This result may be generalized by observing that any desired spectral characteristics can be obtained by filtering a unity spectral level white sequence with the appropriate linear filter [7]. Thus, if the squared magnitude of the frequency response is chosen to be $S_v(\omega)$, the resulting periodogram expressed in terms of $I_{NW}(\omega)$, the periodogram of the white sequence, becomes

$$I_N(\omega) \simeq S_v(\omega)\, I_{NW}(\omega) \tag{22}$$

This expression is not exact because of the transient end effects associated with the filtering of a finite length sequence. However, if the sequence is long compared to the memory of the filter, then Eq. (22) should yield an accurate representation of the actual spectrum. Thus we conclude from Eqs. (21) and (22) that the spectral samples remain independent, with magnitudes that approximate the actual spectral level at that frequency. It has been shown [7] that the variance of the samples is

$$\mathrm{var}\,(I_N(k)) \simeq S_v^2(k)\left\{1 + \left[\frac{\sin(2\pi k)}{N\sin\left(\frac{2\pi k}{N}\right)}\right]^2\right\} \tag{23}$$

from which it follows that for all $k > 0$, the standard deviation of a periodogram sample is equal to the spectral level. The resulting wild fluctuations from one sample to the next render a single periodogram somewhat useless as a spectral level estimator. The problem can be ameliorated by averaging a large number of independent periodograms, as originally proposed by Bartlett. If M independent periodograms are averaged, the variance at any frequency is reduced by M, while the expected value is preserved. Denoting the averaged periodogram samples by $B_N(k)$, we have

$$\lim_{N\to\infty} E\{B_N(k)\} = S_v(k) \tag{24a}$$

$$\mathrm{var}\{B_N(k)\} = M^{-1} S_v^2(k)\,; \qquad k = 1, 2, \ldots, N-1 \tag{24b}$$

The spectral density estimate for the data under consideration is shown in Fig. 4, obtained by averaging 100 independent periodograms of the reconstructed phase detector output. A log-log plot was chosen to facilitate comparison with theory. The agreement with the power-law model is evident in the low frequency regions, while dominance of the white noise component occurs at higher frequencies.

B. Maximum Likelihood Estimator

The maximum likelihood estimator described here processes independent frequency samples to obtain estimates of the desired spectral parameters, namely the coefficient S_1, the exponent α, and the equivalent noise spectral level $N_{0E}/2$. After some preliminary processing, the channel-induced signal distortions were found to be separately accessible from the in-phase and quadrature samples, corrupted by independent additive noise samples. We begin by developing the necessary mathematical models.

Since the final spectral estimates are averages of many independent records, the Central Limit Theorem may be invoked for approximating the density of the frequency samples. Al-

though each spectral sample is the squared magnitude of a complex Gaussian random variable and therefore is chi-squared distributed with two degrees of freedom, the operation of averaging a large number of independent samples transforms the averages to Gaussian random variables with the mean and variance given by Eq. (24). Thus we can model the problem as one of estimating the parameters of a deterministic function g from its noise-corrupted samples y:

$$y(k) = g(k; \mathrm{a}) + n_e(k) \tag{25a}$$

$$g(k; \mathrm{a}) = a1 + a2\left(\frac{k}{NT}\right)^{-a3} \tag{25b}$$

Here $n_e(k)$ is an equivalent noise sample representing the estimation error. While $n_e(k)$ is zero mean, its variance depends on the square of the spectral level and on the number of samples averaged, as in Eq. (24b). Since the frequency samples are assumed to be independent, we can write the joint density of the $N - 1$ samples (excluding the sample at $k = 0$, since this sample cannot possibly obey the power-law relation of Eq. (1)) as

$$p(\mathrm{y}|\mathrm{a}) = \prod_{k=1}^{\frac{N}{2}-1} \exp\left\{-\left(\frac{y(k)-g(k)}{\sqrt{2}\,\sigma(k)}\right)^2\right\} (2\pi\sigma^2(k))^{-1/2} \tag{26}$$

with $\mathrm{y} = (y(1), y(2), \ldots, y((N/2-1))$, $\mathrm{a} = (a1, a2, a3)$. For our case, $\sigma(k) = g(k)/\sqrt{M}$. Taking the natural log, and keeping only those terms that contain the parameters of interest, the "log-likelihood" function becomes

$$\Lambda(\mathrm{y}) = -\sum_{k=1}^{\frac{N}{2}-1}\left\{ln(g(k)) + \frac{M}{2}\left(\frac{y(k)}{g(k)}\right)^2 - M\,\frac{y(k)}{g(k)}\right\} \tag{27}$$

With $a1 = N_{0E}/2$, $a2 = S_1$, and $a3 = \alpha$, the maximum likelihood estimates are those values that simultaneously maximize Eq. (27), for the given observation vector. Equivalently, we can find the minimum of the negative of the log-likelihood function. This we proceeded to do, using the simplex method of function minimization described by Nelder and Mead [8].

C. Results

The following parameter estimates were obtained for the data taken on DOY 357, at an SEP angle of 2.25 degrees: $S_1 = 2.13 \times 10^{-3}\ r^2/\mathrm{Hz}$, $\alpha = 2.186$, and $N_{0E}/2 = 8.77 \times 10^{-4}\ r^2/\mathrm{Hz}$. The exponent compares favorably with theory, which predicts a frequency exponent of less than 8/3 for the phase spectra this close to the Sun. The phase spectral coefficient S_1 is also in order-of-magnitude agreement with the measurements in [5], after our result is extrapolated to S-band (2-GHz) frequencies. The estimates obtained by the ad hoc estimator, which does not take into account the time-varying nature of the closed-loop transfer function, were 7.6×10^{-4} for the white noise component and 3.7×10^{-2} for the phase spectral coefficient, assuming a power-law exponent of 8/3. The importance of our signal reconstruction technique is well demonstrated by this example, since the ad hoc estimate of the spectral coefficient appears to be in error.

The degree of complexity required to evaluate the performance of the maximum likelihood estimator by analytical means, such as the Cramer-Rao bound, is beyond the scope and interest of this article. However, performance can be easily evaluated by simulation techniques. Using the spectral model defined in Eq. (25b) with the parameter values $a1 = 8.77 \times 10^{-4}$, $a2 = 2.13 \times 10^{-3}$, $a3 = 2.186$, and adding an independent Gaussian noise sample with the proper variance to each frequency sample, parameter estimates were obtained for 1000 independent simulated spectral densities. The sample means agreed well with the modeled values, indicating that unbiased estimates were obtained. With obvious notation, the standard deviations of the estimation errors were $\sigma_{a1} = 9.3 \times 10^{-6}$, $\sigma_{a2} = 9.5 \times 10^{-5}$, and $\sigma_{a3} = 4.7 \times 10^{-2}$. Therefore the simulations indicate very good accuracy in the final estimates. We must remember, however, that our underlying model is only approximate, since we have assumed a single power-law component to the phase spectrum where in fact there may have been two. In addition, other sources of error in preprocessing the data, such as the use of inaccurate amplitude estimates, were not taken into account in the simulations. However, we did succeed in demonstrating a useful technique for reconstructing phase spectra from observables corrupted by random amplitude effects.

V. Conclusions

Recently, the JPL Advanced Receiver was used to track Voyager 2 as it passed behind the solar corona. During tracking, severe fluctuations were noted in the amplitude of the received signal, particularly at small SEP angles. Since these fluctuations introduced a corresponding random variation into the transfer function of the tracking loop, previous spectral density estimation techniques that assumed a time-invariant loop became inadequate. Thus, a method was developed to extract the desired parameters from the recorded data, taking into account the fluctuating signals.

Our approach is based on the observation that random variations in the transfer function could be attributed directly to the fluctuating amplitude, suggesting the use of a time-varying inverse filter to remove these unwanted amplitude effects from

the phase-detector output. This required estimates of the random amplitude. Since both in-phase and quadrature samples were recorded, the necessary amplitude estimates could be obtained from the in-phase samples, provided the loop remained in lock. Thus, we were able to recover the phase error process from the phase-detector output by means of a time-varying inverse filter operation. Subsequent spectral analysis and parameter estimation yielded results that agreed both with theory and with measurements made independently by other researchers, confirming the validity of our approach.

The ability to obtain real-time estimates of the random amplitude function along with the relevant phase and noise spectral parameters opens up the possibility of adaptive control, where the system parameters are continuously adjusted to achieve optimum performance. This would be useful whenever significant amplitude variations occur, as with a wobbling spacecraft antenna, mechanical vibrations at the receiving antenna, solar plasma effects, tropospheric turbulence, etc. Perhaps a rudimentary form of an adaptive system could be demonstrated during the upcoming solar occultation of Voyager 2, in January of 1989. Such a demonstration might have a significant impact on future centimeter and millimeter wave DSN system design, where fluctuations in received signal strength due to atmospheric effects may be routinely encountered.

References

[1] V. A. Vilnrotter, W. J. Hurd, and D. H. Brown, "Optimized Tracking of RF Carriers With Phase Noise, Including Pioneer 10 Results," *TDA Progress Report 42-91*, vol. July–September 1987, Jet Propulsion Laboratory, Pasadena, California, pp. 141–157, November 15, 1987.

[2] D. H. Brown and W. J. Hurd, "DSN Advanced Receiver: Breadboard Description and Test Results," *TDA Progress Report 42-89*, vol. January–March 1987, Jet Propulsion Laboratory, Pasadena, California, pp. 48–66, May 15, 1987.

[3] D. H. Brown, W. J. Hurd, V. A. Vilnrotter, and J. D. Wiggins, "Advanced Receiver Tracking of Voyager 2 Near Solar Conjunction," *TDA Progress Report 42-93*, vol. January–March 1988, Jet Propulsion Laboratory, Pasadena, California, May 15, 1988.

[4] J. W. Armstrong et al., *The Deep Space Network – A Radio Communications Instrument for Deep Space Exploration*, JPL Publication 82-104, Jet Propulsion Laboratory, Pasadena, California, July 15, 1983.

[5] R. Woo and J. W. Armstrong, "Spacecraft Radio Scattering Observations of the Power Spectrum of Electron Density Fluctuations in the Solar Wind," *J. Geophys. Res.*, vol. 84, no. A12, pp. 7288–7296, 1979.

[6] R. Gagliardi, *Introduction to Communications Engineering*, New York: John Wiley & Sons, 1978.

[7] A. V. Oppenheim and R. W. Schafer, *Digital Signal Processing*, Englewood Cliffs, New Jersey: Prentice-Hall, 1975.

[8] J. A. Nelder and R. Mead, "A Simplex Method for Function Minimization," *Computer J.*, vol. 7, pp. 308–313, 1965.

[9] S. Aguirre and W. J. Hurd, "Design and Performance of Sampled Data Loops for Subcarrier and Carrier Tracking," *TDA Progress Report 42-79*, vol. July–September 1984, Jet Propulsion Laboratory, Pasadena, California, pp. 81–95, November 15, 1984.

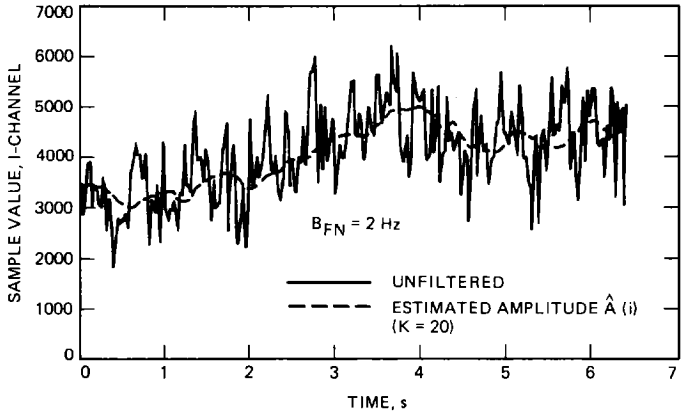

Fig. 1. Sample sequence of resampled observables: I-channel

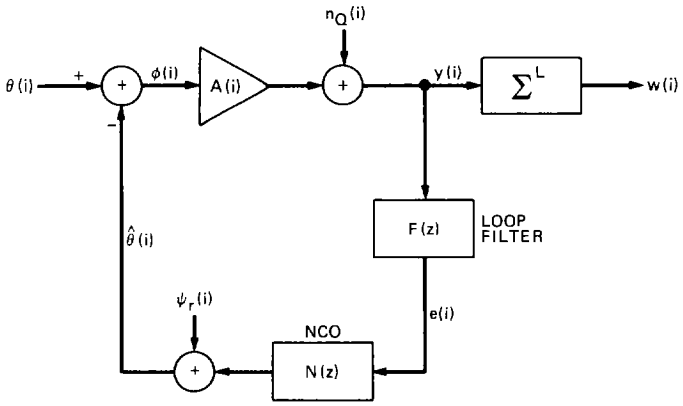

Fig. 3. Linear model of time-varying digital phase-locked loop

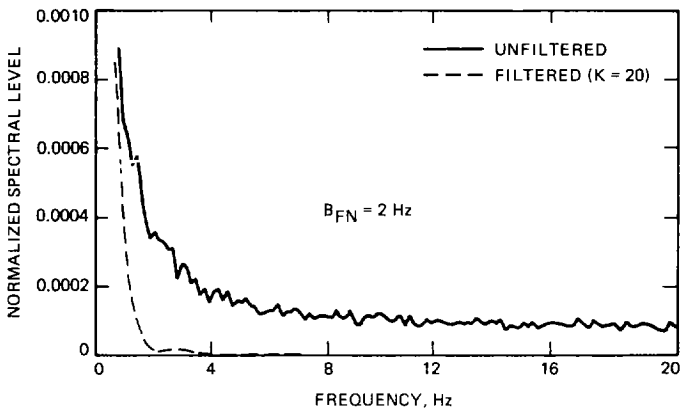

Fig. 2. Normalized spectral density estimates of amplitude fluctuations

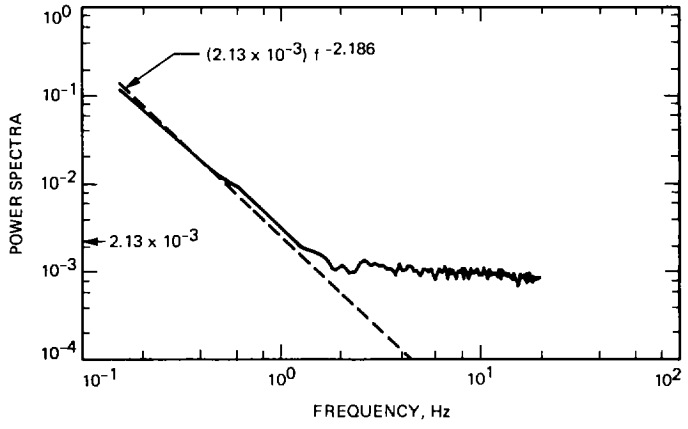

Fig. 4. Estimated power spectral density of reconstructed observables

Appendix

Derivation of the Coefficients for the Inverse Filter, *P*(z)

The coefficients of Eq. (12b) are derived.

From equation (12) of [9],

$$G(z) = AKF(z)N(z)$$

$$= \frac{\frac{r}{2}(z+1)\left[\frac{4B_L T}{r+1}(z-1)+\left(\frac{4B_L T}{r+1}\right)^2 z\right]}{(z-1)^2 z^2} \tag{A-1}$$

Let us assume that the variation in $A(i)$ is slow relative to the response time of the loop, which was the case in our experiment. Thus, for short intervals we can use the approximation

$$A(i) \simeq AK$$

By Eq. (12a),

$$P(z) = \frac{[1+G(z)]}{AK} \tag{A-2}$$

so

$$P(z) = \frac{\left[\dfrac{1-2z^{-1}+\left[\frac{r}{2}(d+d^2)+1\right]z^{-2}+\frac{r}{2}d^2 z^{-3}-\frac{r}{2}dz^{-4}}{1-2z^{-1}+z^{-2}}\right]}{AK} \tag{A-3}$$

where

$$d = \frac{4B_L T}{r+1}$$

Designating the input and output of $P(z)$ as $Y(z)$ and $V(z)$, respectively, we have

$$P(z) = \frac{V(z)}{Y(z)} \tag{A-4}$$

Then from (A-3) and (A-4),

$$V(z)[1-2z^{-1}+z^{-2}] = Y(z)\left[1-2z^{-1}+\left[\frac{r}{2}(d+d^2)+1\right]z^{-2}+\frac{r}{2}d^2 z^{-3}-\frac{r}{2}dz^{-4}\right] \tag{A-5}$$

Taking the inverse Z transform,

$$v(k)-2v(k-1)+v(k-2) = y(k)-2y(k-1)+\left[\frac{r}{2}(d+d^2)+1\right]y(k-2)+\frac{r}{2}d^2 y(k-3)-\frac{r}{2}dy(k-4) \tag{A-6}$$

Solving for $v(k)$ yields

$$v(k) = y(k)-2y(k-1)+\left[\frac{r}{2}(d+d^2)+1\right]y(k-2)-\frac{r}{2}d^2 y(k-3)-\frac{r}{2}dy(k-4)+2v(k-1)-v(k-2) \tag{A-7}$$

The coefficients of Eq. (12a) can be obtained by inspection from Eq. (A-7).